

1 **Nash et al. Author response**

2

3 **Changes made for minor grammatical and typos as requested.**

4

5 Comments:

6 L 34 – need to define CCA again

7 L34 – into > in

8 L37 – decreases > decrease

9 L 42 – move this definition up to L 34 and remove it from here

10 L 52 magnesium > Mg (and throughout)

11 L 80 epithallus > epithelial

12 *Above changes made*

13 Paragraph starting at L86 – be more explicit – are you talking about dolomite in general or in
14 CCA?

15 *Paragraph revised*

16

17 L 97 ; and 3)

18 L153 – be more precise when describing XRD sampling (how did you mill off powder – sample
19 size, etc)

20 *Details added*

21

22 L182, 184, and further – do not write CCA before the species name each time.

23 *Changed*

24

25 L198 However,

26 L202 Therefore,

27 L215 However,

28 The manuscript is loaded with conjunctive adverbs which are almost always missing a comma.

29 Please fix.

30 *Commas added and some sentences reworded to remove the conjunctive adverbs..*

31

32 L336 – and more specifically, species specific

33 *Species included.*

34

35

36

37

38

39

40

41 **Ocean acidification does not affect magnesium composition or dolomite**

42 **formation in living crustose coralline algae, *Porolithon onkodes* in an**

43 **experimental system**

44 Nash, M.C.^{1*} Uthicke², S, Negri², A. P., Cantin², N. E.
45 ¹Research School of Physics, Australian National University
46 ²Australian Institute of Marine Science, Townsville, Queensland
47 *corresponding author: merinda.nash@anu.edu.au

48

49 **Abstract**

50 There are concerns that Mg-calcite crustose coralline algae (CCA), which are key reef
51 builders on coral reefs, will be most susceptible to increased rates of dissolution under
52 higher pCO₂ and ocean acidification. Due to the higher solubility of Mg-calcite, it has
53 been hypothesized that magnesium concentrations in CCA Mg-calcite will decrease as
54 the ocean acidifies, and that this decrease will make their skeletons more chemically
55 stable. In addition to Mg-calcite, CCA *Porolithon onkodes* the predominant encrusting
56 species on tropical reefs, can have dolomite (Ca_{0.5}Mg_{0.5}CO₃) infilling cell spaces which
57 increases their stability. However, nothing is known about how bio-mineralised dolomite
58 formation responds to higher pCO₂. Using *P. onkodes* grown for 3 and 6 months in tank
59 experiments, we aimed to determine 1) if mol% MgCO₃ in new crust and new settlement
60 was affected by increasing CO₂ levels (365, 444, 676 and 904µatm), 2) whether bio-
61 mineralised dolomite formed within these time frames, and 3) if so, whether this was
62 effected by CO₂. Our results show there was no significant affect of CO₂ on mol%
63 MgCO₃ in any sample set, indicating an absence of a plastic response under a wide range
64 of experimental conditions. Dolomite within the CCA cells formed within 3 months and
65 dolomite abundance did not vary significantly with CO₂ treatment. While evidence
66 mounts that climate change will impact many sensitive coral and CCA species, the results
67 from this study indicate that reef-building *P. onkodes* will continue to form stabilising
68 dolomite infill under near-future acidification conditions, thereby retaining its higher
69 resistance to dissolution.

70

71 **1 Introduction**

72 Determining the influence of ocean acidification from increasing CO₂ concentrations on
73 mineral formation of crustose coralline algae (CCA) is not only important to understand
74 potential changes in CCA and their reef building capacity in the future, but also to

Rob Nash 6/9/15 4:05 PM

Deleted: to

76 understand the past. As atmospheric carbon dioxide (CO₂) concentrations increase,
77 fundamental changes to the ocean's chemistry follow. Seawater pH and the carbonate
78 saturation state (Ω) decrease, thus increasing the solubility of CaCO₃ skeletons. Current
79 projections are that by the end of this century, if anthropogenic CO₂ emissions continue
80 unabated, tropical surface seawater pH will drop by 0.3-0.4 units to ~ pH 7.8 (Orr 2011).
81 Marine organisms forming carbonate skeletons are susceptible to increased rates of
82 dissolution as pH declines (reviewed in Howard et al., 2012). There are concerns that
83 CCA will be one of the first reef-building organisms to suffer as CO₂ rises (e.g. Diaz-
84 Pulido et al., 2012), due to the higher solubility of their skeleton. The possibility has also
85 been raised that CCA may decrease their uptake of Mg to form more stable lower Mg-
86 calcite in response to higher CO₂ concentrations (e.g. Andersson et al., 2008; Ries 2011).
87
88 Experimental data on the impacts of pH on Mg uptake by tropical CCA are limited. The
89 branching coralline *Neogoniolithon* demonstrated a decreased magnesium concentration
90 in severely low pH conditions (Ries 2011). However, CCA *Porolithon onkodes*
91 transplanted into low pH treatments for 8 weeks did not exhibit any Mg composition
92 change with pH in new surface tissue (Diaz-Pulido et al., 2014). Temperate coralline
93 *Corallina elongate* had a variable response with new growth on existing branches not
94 exhibiting a response to elevated CO₂ whereas new structures grown during the
95 experiment did have decreased Mg content in higher CO₂ treatments (Egilsdottir et al.,
96 2012). Temperate rhodoliths *Lithothamnion glaciale* did not change Mg content in
97 different CO₂ treatments while living. However, a significant decrease in the Mg content
98 in low pH compared to dead thalli in the same treatment raised the possibility that there
99 was a biological response (Kamenos et al., 2013). Recently it was discovered that tropical
100 CCA *P. onkodes* commonly possess additional Mg minerals dolomite (Mg_{0.5}Ca_{0.5}CO₃)
101 and magnesite (MgCO₃) infilling cells in the crust (Nash et al., 2011). This additional
102 mineralisation significantly reduces rates of skeletal dissolution compared to *P. onkodes*
103 without dolomite cell infill (Nash et al., 2013a). A combination of high CO₂ and
104 increased temperature over 8 weeks led to a ~300% increase in the relative quantity of
105 dolomite in *P. onkodes* crust transplanted into the treatment conditions (Diaz-Pulido et
106 al., 2014). This was due to endolithic cyanobacteria, *Mastigocoleus* sp, removing calcium

Rob Nash 6/9/15 4:04 PM

Deleted: s

Rob Nash 6/9/15 4:06 PM

Deleted: Mg-calcite crustose coralline algae (CCA)

Rob Nash 6/9/15 4:33 PM

Deleted: magnesium

Rob Nash 6/20/15 3:26 PM

Deleted: magnesium

Rob Nash 6/20/15 3:27 PM

Deleted: experimental

Rob Nash 6/9/15 4:06 PM

Deleted: magnesium

Rob Nash 6/20/15 3:28 PM

Deleted: ,

Rob Nash 6/20/15 3:28 PM

Deleted: h

Rob Nash 6/20/15 3:28 PM

Deleted: magnesium

117 from the Mg-calcite skeleton but not from dolomite, leading to destruction of Mg-calcite
118 and a relative increase in dolomite. It could not be determined if there was also an
119 increase in the formation of primary dolomite.

120

121 When CCA grow to form the thick crust crucial to cementing together the structural reef
122 framework, the new growth extends upwards leaving the old growth as a white crust
123 without pink photosynthetic pigment. The pink surface of the CCA is the epithallus and
124 the pink colouration is due to the presence of pigmented photosynthetic tissue within the
125 Mg-calcite skeleton. In other species of corallines, this pink surface has been shown to
126 slough off (Pueschel et al., 2005) and be grazed by chitons and limpets (Adey et al.,
127 2013). The white crust underneath (perithallus) has been shown in other species of CCA
128 to form as cell by cell growth downward from the meristem cells (growth layer between
129 epithallus and perithallus) (Adey et al., 2013). Thus the white crust is a product of

130 meristem growth, and not a build up of epithelial growth after it loses its pigmentation

131 It is in this important reef-structure forming white crust that dolomite infill is abundant
132 (Nash et al., 2011; Diaz-Pulido et al., 2014). As yet, there have been no experiments to
133 determine the impact of CO₂ levels on mol% MgCO₃ and dolomite formation in the white
134 crust grown in differing CO₂ treatments.

135

136 There is a noted correlation of sedimentary dolomite abundance and greenhouse
137 conditions (high temperature, high CO₂) over the geological past (e.g. MacKenzie et al.,
138 2008; Wilkinson and Given 1986). To understand the past, it is necessary to separate the
139 roles that CO₂ and temperature may have had on constraining dolomite concentration.

140 Bio-mineralised dolomite has been found in modern environments (Vasconcelos and
141 Mackenzie 1997; Nash et al., 2011), but it is not known how changes in CO₂

142 concentrations may affect formation of bio-mineralised dolomite. This study describes
143 the first experiments that constrain the role of CO₂ on CCA bio-mineralised dolomite
144 formed in differing CO₂ environments.

145

146 The aims of this investigation were threefold; 1) to identify any changes in mol% MgCO₃
147 in new settlement and new white crust of *P. onkodes* grown in Pre-industrial, Control

Rob Nash 6/9/15 6:01 PM

Deleted: h

Rob Nash 6/9/15 4:47 PM

Deleted: allus

Rob Nash 6/20/15 3:24 PM

Deleted: formation

Neal Cantin 6/12/15 8:35 AM

Deleted: forming

Neal Cantin 6/12/15 8:35 AM

Deleted: levels

153 (present day), Medium (near future) and High (end of century) CO₂ (IPCC, 2007)
154 conditions over 3 and 6 months; 2) to determine whether [CCA](#) bio-mineralised dolomite
155 is formed within these timeframes; 3) to determine if the CO₂ concentration affects [CCA](#)
156 bio-mineralised dolomite formation.

157

158 **2 Methods**

159 **2.1 Experiment**

160 Fragments of live *P. onkodes* were collected from the upper reef crests (2 – 3 m depth) of
161 Davies Reef (18°49.29'S, 147°37.99'E), Great Barrier Reef in August 2012. To
162 eliminate open carbonate surfaces, CCA chips (~1 cm diameter) were sealed around the
163 sides and base in non-toxic under water glue (Mr. Sticky's, Fair Oaks, CA) and attached
164 to PVC slides (only the top live surfaces were exposed to seawater). Blank slides were
165 also added to the system to identify and track new CCA settlement. Slides were mounted
166 in custom perspex holders which were held in place on aquarium walls using magnets.
167 The experimental system used was described in (Uthicke et al., 2013). Briefly, fresh
168 filtered seawater (0.4 mm) was added to three replicate tanks (for each treatment)
169 replacing the water twice daily. Flow rates in each experimental tank were 12 L min⁻¹. In
170 addition to a present day (pH_T 8.0 target, measured mean 7.96 +/- 0.04 SE CO₂: 444 +/-
171 37 [µatm](#)), mid-century 2050 (future pH_T 7.9 target, measured mean 7.90 +/- 0.04 SE CO₂:
172 676 +/- 37 [µatm](#)) and end of century 2100 (future pH_T 7.75 target, measured mean 7.77
173 +/- 0.06 SE CO₂ 904 +/- 32 [µatm](#)) target acidification treatments, this experiment also
174 included a pre-industrial treatment (past pH_T 8.14 target, measured mean 8.09 +/- 0.04 SE
175 CO₂: 365 +/- 37 [µatm](#)). Acidified treatments were achieved by bubbling CO₂ into sump
176 tanks with solenoid valves (SMC pneumatics) and [controlled with](#) pH setpoints, while the
177 pre-industrial treatment was achieved by passing a stream of [atmospheric](#) air through 2
178 soda lime canisters and mixing the low CO₂ scrubbed air with the incoming seawater in a
179 counter current exchange tower prior to flowing into each experimental tank.
180 Temperatures were controlled (Avg. 26.1 ± 0.15°C) with a heater chiller unit (EvoHeat
181 DHP40). pH and temperature were monitored continuously (30 sec sampling rate) with
182 ISFET type pH probes (Endress Hauser CPS-471D). Seawater CO₂ concentrations were
183 measured using a LiCor (LI-840A) CO₂/H₂O analyser. This experiment was conducted

Neal Cantin 6/12/15 9:35 AM

Deleted: ppm

Rob Nash 6/20/15 3:25 PM

Deleted:

186 within the outdoor aquarium facility at the Australian Institute of Marine Science under
187 natural daily light cycles during the Austral summer (October-April). Outdoor light
188 intensities were reduced with 70% UV blocking green shade cloth to an average intensity
189 of $210 \pm 12 \mu\text{mol photons m}^{-2} \text{ s}^{-1}$, with a daily maximum of $330 \mu\text{mol photons m}^{-2} \text{ s}^{-1}$.
190 These light intensities correspond to the daily average light intensity on shallow reefs.
191

192 2.2 Sample selection

193 Subsets of CCA's in resin were removed from the tanks after 3 and 6 months. The
194 settlement slides were removed after 6 months. Samples were randomly selected from
195 these for XRD analyses. New crust from the resin-embedded CCA's was sampled by
196 breaking off [the](#) crust that overgrew the resin. This ensured that only crust formed during
197 the experiment was included in the new crust analyses. The new crust typically had a thin
198 layer (~0.5 to 2 mm) of white crust overlain by a layer of pink photosynthetic epithallus
199 (Figure 1). CCA that had settled on the plastic slides after 6 months had only pink crust
200 and there was no white crust underneath. Typically for the new settlement CCA, 2-4
201 settlement patches were required to obtain sufficient material for analysis by XRD, thus
202 [each individual result for new settlement is an average of several CCA patches.](#) These
203 CCA had not reached reproductive stage and could not be identified. For the 6 month
204 experiment, CCA's in resin from the control tanks were unavailable for mineral analysis.

205 2.3 Analyses

206 CCA were cut using a bench-top saw with a 2 mm thick diamond impregnated blade. A
207 slice through the middle of each 3-month sample was kept for SEM. Scanning Electron
208 Microscopy-Energy Dispersive Spectroscopy (SEM-EDS) was undertaken at the
209 Australian National University using a Zeiss UltraPlus field emission scanning electron
210 microscope (FESEM) equipped with an HKL electron backscatter diffraction (EBSD)
211 operated at 15kV, 11 mm working distance. CCA were mounted using carbon tape and
212 carbon coated. Subsampling for XRD was taken from the matching side of the remainder
213 crust. [Samples \(>20 mg\) were milled by hand in an agate mortar. Fluorite was added as](#)
214 [an internal standard. Acetone was not used as this has been found to react with the pink](#)
215 [pigmented surface samples. Samples were mounted onto quartz low background holders.](#)
216 [Scan range was 25-33° 2-theta, step size 0.02° 2-theta and a scan speed of 1°/min. Xray](#)

Rob Nash 6/9/15 5:58 PM

Deleted:

Neal Cantin 6/15/15 8:55 AM

Deleted: .

Neal Cantin 6/15/15 9:31 AM

Deleted: d

220 diffraction and mineral determination was carried out following Nash et al., (2013b).
221 Simply, this method uses the asymmetry off the higher 2-theta side of the Mg-calcite
222 XRD peak to detect dolomite. The more asymmetry the greater proportion of dolomite in
223 the crust. A shoulder off the higher 2-theta side of the peak indicates magnesite (MgCO_3)
224 is also present. This asymmetry and shoulder is captured with the asymmetry mol%
225 measurement. The asymmetry mol% is used to compare for differences in relative
226 dolomite and magnesite quantities (Nash et al., 2013b). It is not a measurement of
227 absolute quantity. However, when compared to mineral quantities determined using
228 standard curve fitting techniques, the differences in asymmetry well reflect the
229 differences in dolomite and magnesite quantities (as used in Diaz-Pulido et al., 2014).
230 See Figure 1 (Supplement) for example scans.

Rob Nash 6/20/15 3:36 PM

Deleted: ,

Rob Nash 6/20/15 3:36 PM

Deleted: h

231 232 **2.4 Dolomite terminology**

233 Stoichiometric dolomite is 50 mol% MgCO_3 . Typically dolomite formed under high
234 temperature is stoichiometric and well ordered (Kaczmarek and Sibley 2011). Ordering
235 occurs where there are alternating layers of MgCO_3 and CaCO_3 in the calcite lattice,
236 whereas completely disordered dolomite has Mg randomly substituting for Ca in the
237 lattice. Sedimentary dolomite formed at sea surface temperature and pressure and not
238 subject to post-deposition burial and metamorphism, typically is non-stoichiometric with
239 a range of 37.5 to 52 mol% MgCO_3 (Jones et al., 2001) and not well ordered (Kaczmarek
240 and Sibley 2011). Synthetically formed disordered dolomite has been shown to be
241 unstable in aqueous solutions and therefore it is thought that disordered dolomite cannot
242 form or persist in the open marine environment in which sedimentary dolomite forms
243 (Gaines 1977). A variety of descriptions exist for dolomite that deviates from
244 stoichiometric and perfectly ordered; non-ideal, poorly ordered or disordered,
245 protodolomite, pseudo-dolomite and calcium enriched dolomite (Gaines 1977).

246
247 Here we use the term dolomite to represent magnesium calcite in the range 38-62 mol%
248 MgCO_3 , as measured for *P. onkodes* dolomite (Nash et al., 2011) without inferring cation
249 ordering status, that is, whether it is ordered, disordered or partially ordered. The *P.*
250 *onkodes* dolomite has previously been demonstrated via etching experiments and natural

Rob Nash 6/9/15 5:35 PM

Deleted: CCA

Rob Nash 6/9/15 5:35 PM

Deleted: CCA

255 dissolution processes to have a delayed dissolution reaction compared to Mg-calcite and
256 has different crystal forms to Mg-calcite (Nash et al., 2013a). Furthermore, it has been
257 documented that Mg-calcite in *P. onkodes* ranges up to ~26 mol% MgCO₃ (Nash et al.,
258 2011) and there is a well-defined division from dolomite which commences at ~38 mol%
259 MgCO₃. Experimental work has demonstrated that cyanobacteria (*Mastigocoleus* sp)
260 which bio-erode limestone by removing calcium, do not take calcium from dolomite rock
261 (Ramirez-Reinat and Garcia-Pichel 2012). Experiments on live dolomite-forming *P.*
262 *onkodes* also show that the same cyanobacteria remove calcium from Mg-calcite but do
263 not remove calcium from the *P. onkodes* dolomite. *P. onkodes* Mg-C and *P. onkodes*
264 dolomite have distinctly different physical properties and *P. onkodes* dolomite reacts
265 under chemical (Nash et al., 2013a) and bio-erosion conditions (Diaz-Pulido et al., 2014)
266 comparably to dolomite the rock. We have been unable to confirm the presence of
267 ordering peaks by XRD for the dolomite within the living *P. onkodes* (Nash et al.,
268 2013b). However, the persistence of the CCA dolomite in aqueous environments and its
269 greater resistance to dissolution than Mg-calcite (Nash et al., 2013a) suggests there is
270 some degree of ordering and *P. onkodes* dolomite is not the same mineral as Mg-calcite
271 which theoretically becomes less stable with greater Mg-substitution (Andersson et al.,
272 2008). Therefore, we consider that referring to the CCA mineral as dolomite, with the
273 caveat that this is without inferring cation-ordering status is the most appropriate
274 identification for the mineral at this time. Our decision to use this terminology for Mg-C
275 > 38 mol % MgCO₃ is supported by recently published clarification on terminology for
276 Ca-Mg carbonates (Zhang et al., 2015).

277

278 **2.5 Crust terminology**

279 The term 'pre-experimental growth' refers to crust grown in situ at Davies reef prior to
280 collection for the experiment. The new crust (experimental) is the growth above the
281 height of the resin. The 'new crust' terminology is used because this includes both the
282 white crust of the perithallus and the pink surface epithallus. There may also be re-
283 growths within the white crust that includes hypothelial cells and alteration to aragonite
284 (see for example Fig. 8). The new settlement on slides in the 6 month treatment was

Rob Nash 6/9/15 5:35 PM
Deleted: CCA

Rob Nash 6/9/15 5:35 PM
Deleted: CCA

Rob Nash 6/9/15 5:35 PM
Deleted: CCA

Rob Nash 6/9/15 5:36 PM
Deleted: CCA

Rob Nash 6/9/15 5:39 PM
Formatted: Subscript

Rob Nash 6/9/15 6:02 PM
Deleted: ,

Rob Nash 6/9/15 6:09 PM
Formatted: Font:Bold

Rob Nash 6/9/15 6:09 PM
Formatted: Font:Bold

Rob Nash 6/9/15 6:08 PM
Deleted: allus

291 | predominantly pink indicating epithelial growth. However, when CCA settle, the first
292 | cells laid down are hypothelial cells growing lengthways parallel to the surface and then
293 | vertical growth of the epithallus, followed by the perithallus (Steneck 1986). A scraping
294 | sample would include not only epithallus but also minor hypothallus and possibly the
295 | start of a perithallus. For this reason we use the term new settlement rather than epithallus
296

Rob Nash 6/9/15 6:07 PM

Deleted: allus

Rob Nash 6/9/15 6:08 PM

Deleted: allus

297 | **2.5 Statistical analysis**

298 | We tested for differences between CO₂ treatments and sample type using two factor
299 | analysis of variance (ANOVA). Different CO₂ treatments (Factor Treatment) and
300 | experimental growth versus pre-experimental growth (Factor Type) were both used as
301 | fixed factors. Residual plots and boxplots confirmed that there were no deviations from
302 | ANOVA assumptions. Because slightly unequal sample sizes were used in each
303 | treatment, we applied marginal sums of squares for the F-tests.
304

305 | **3 Results**

306 | **3.1 Mineral composition in different CO₂ treatments**

307 | We investigated the mineral composition of CCA exposed to different OA conditions for
308 | 3 and 6 months in a long-term aquarium experiment. There were no significant
309 | differences in mineral composition between any of the CO₂ treatments (Table 1). For the
310 | new *P. onkodes* crust formed during the 3 month duration (Figure 2a), the mol% MgCO₃
311 | range is 16.4 – 16.7 mol% MgCO₃ (n = 5 per treatment, averages: Pre 16.6, Control 16.5,
312 | Medium 16.4, High 16.7 mol% MgCO₃) (full results supplement Table 1). This range is
313 | only 0.1 mol% more than measurement precision (Nash et al., 2011). For the new *P.*
314 | *onkodes* crust formed over 6 months (Fig. 2b), the mol% MgCO₃ range was the same as
315 | the 3 month crust 16.4 – 16.7 mol% MgCO₃, (Pre 16.7 n=5, Medium 16.4 n=3, High 16.5
316 | mol% MgCO₃ n=6) (Supplement Table 2). Many of the Mg-calcite XRD peaks for both
317 | the 3 and 6 month crust demonstrated asymmetry indicating the presence of dolomite (as
318 | per Nash et al., 2011, 2012, 2013a,b, Diaz-Pulido et al., 2014). There was no significant
319 | difference in the dolomite asymmetry related to CO₂ treatments (asymmetry test, Table
320 | 1). For unidentified CCA that had settled on the slides over 6 months (Fig. 2c),
321 | (Supplement Table 3) the mol% MgCO₃ ranged from 14.7- 14.9 (Pre 14.8 n=3, Control

Rob Nash 6/20/15 3:37 PM

Deleted: however

Rob Nash 6/20/15 3:37 PM

Deleted: t

326 n=4 14.7, Medium 14.7 n=5, High 14.9 mol% MgCO₃ n=5). The new settlement CCA
327 did not have dolomite, i.e. no peak asymmetry, consistent with the absence of white crust
328 underneath.

329

330 **3.2 Mineral compositional differences between crust layers**

331 As there was no significant difference between treatments, all treatments were combined
332 for each time period. There was a significant difference in Mg composition between
333 experimental crust and pre-experimental crust. Mg-calcite mol% MgCO₃ was also
334 significantly different for new settlement (pigmented growth without development of
335 white crust) compared to new crust (growth that has developed white crust). The 6 month
336 new settlement (pigmented growth only) at 14.8 mol% MgCO₃ (Fig. 3) was significantly
337 lower than the mol% MgCO₃ for the new crusts from the 3 and 6 months new crusts
338 (~16.5 mol% MgCO₃). The asymmetry indicating dolomite presence was absent from the
339 new growth, but appeared in new white crust within 3 months (Asymm mol % 17.6) and
340 was higher again for the 6 month new crust (Asymm mol % 18.7). The mol% MgCO₃
341 and asymmetry mol% in the pre-experimental *P. onkodes* crust (the crust formed in the
342 natural environment prior to sample collection) were even higher at 17.5 and 21.6 mol%
343 MgCO₃ respectively (Fig. 3) (full data Supplement Table 4).

344

345 **3.3 SEM results**

346 **3.3.1 Comparison of crust across treatments and experimental / pre-experimental**

347 Although there was no detected difference in mineral composition across treatments,
348 SEM was undertaken to visualise potential differences in calcification structures between
349 treatments. There was no visible difference in calcified crust detected between CCA from
350 pre-industrial, control or high CO₂ treatments. There was however, a clear difference
351 in the structure of the crust grown during the experimental duration compared to the pre-
352 experimental crust (Figs. 4, 5 and supplement Fig. 2). This difference was observed in
353 control CCA, as well as pre-industrial and high CO₂ CCA indicating the difference was
354 not related to the CO₂ levels. Crust formed during the experiment appeared less
355 organized and also appeared structurally less dense (Fig. 6) with cracks and associated
356 gaps in the crust that were not present in the pre-experimental crust. The difference in

Rob Nash 6/20/15 3:38 PM

Deleted: magnesium

358 density was based on observation and not able to be quantified.

359

360 The experimental crust had compressed under the action of the saw used to slice the CCA
361 (Fig. 7). We note that this compression by the saw would have made it difficult to
362 identify any differences in growth structure between the CO₂ treatments. Previous work
363 relying on SEM for CCA interpretation has used both saw cutting similarly to here (Nash
364 et al., 2011, 2013a, b; Diaz-Pulido et al., 2014) as well as fracturing without any further
365 treatment of the sample (Nash et al 2013a, Diaz-Pulido et al., 2014). There has not been
366 an observed impact of saw cutting on experimental samples (Diaz-Pulido et al., 2014).
367 However, those previous samples were polished after cutting and fine cracks may have
368 been less obvious due to polishing. The crust features in the pre-experimental crust are
369 comparable to features in other *P. onkodes* analysed using SEM that have been cut, cut
370 and polished or only fractured (Nash et al., 2011, 2013a,b; Diaz-Pulido et al., 2014) and it
371 is unlikely that the use of the saw has introduced an artifact into this study other than to
372 highlight the susceptibility of the experimental crust to crushing compared to pre-
373 experimental crust.

374

375 3.3.2 Dolomite features

376 Dolomite composition determined by SEM-EDS ranged from 37.3 to 59.8 mol% MgCO₃
377 (Table 5 Supplement), comparable to the range identified in previous studies (Nash et al.,
378 2011). There was a de-lination along the new experimental growth where dolomite was
379 nearly absent compared to consistent infill in pre-experimental crust (Figs 5-7,
380 Supplement Fig. 3). The structure of dolomite formed in the experimental crust also
381 appeared different to that which formed in the pre-experimental crust (Fig. 4). New
382 growth dolomite did not generally fill the cells as was observed in the pre-experimental
383 growth. In the experimental growth, dolomite was present as lumpy infill or lining (Fig.
384 4 a and b). In the pre-experimental crust, dolomite lined and in-filled most cells (Fig. 4 c
385 and d). In the control CCA the pre-experimental crust had an opaque organic film that
386 was not visible in experimental growth (Fig. 5c), although there was organic material in
387 the cells (Supplement Fig. 3).

388

Rob Nash 6/20/15 3:41 PM

Deleted:

Rob Nash 6/20/15 3:41 PM

Deleted: h

Rob Nash 6/9/15 5:37 PM

Deleted: CCA

Rob Nash 6/20/15 3:42 PM

Deleted:

393 **3.3.3 Crust damage possibly due to transfer to experimental tanks**

394 Pre-experimental crust immediately below experimental growth had aragonite cell infill
395 (Fig. 7). In previous work aragonite infill of this type has only been observed at the base
396 of the CCA crust exposed to seawater (Nash et al., 2013a Supplement), or in parts of the
397 skeleton that have been damaged allowing seawater to penetrate. However, we could find
398 no obvious signs of damage to the crust. *P. onkodes* has varied mineralogy throughout the
399 pre-experimental crust (Fig. 8) with patches altered to aragonite and dolomite bands.
400 Regrowth in damaged areas within the pre-experimental crust was more dolomite rich
401 than surrounding areas (Fig. 8b) indicating that damage to crust in the open environment
402 had not resulted in a reduction in dolomite formation.

Rob Nash 6/9/15 5:38 PM

Deleted: CCA

404 **4 Discussion**

405 Our results show that over the experimental duration 1) there were no changes in any
406 crust mineral composition relating to CO₂ concentrations; 2) CCA bio-mineralised
407 dolomite forms within 12 weeks within aquarium conditions; and 3) CO₂ concentrations
408 do not affect CCA bio-mineralised dolomite formation.

410 **4.1 Magnesium composition and calcification processes**

411 The higher mol% MgCO₃ for white crust compared to the pigmented new growth layer
412 (new settlement) has been documented previously for *P. onkodes* (Diaz-Pulido et al.,
413 2014). This higher mol% MgCO₃ in the white crust suggests that controls on magnesium
414 uptake are different for the white crust (perithallium) than the pigmented surface layers
415 (epithallium).

416
417 Considering that CCA crusts are increasingly being used for paleo environmental
418 reconstruction (e.g. Kamenos et al., 2008; Halfar et al., 2013; Caragnano et al., 2014;
419 Darrenougue et al., 2014; Fietzke et al., 2015), it is important to know whether this
420 difference in Mg composition between the pigment surface and white crust is part of the
421 standard calcification processes of the *P. onkodes* or due to post-depositional change. In
422 this and previous work (Nash et al., 2011, 2013a) portions of the crust that have been

Rob Nash 6/20/15 3:43 PM

Deleted: magnesium

Rob Nash 6/20/15 3:17 PM

Deleted: CCA

Rob Nash 6/20/15 3:18 PM

Formatted: Font:Italic

426 diagenetically altered post-deposition have cells in-filled by aragonite or Mg-calcite.
427 Typically the cell walls have not exhibited evidence of alteration even when there has
428 clearly been exposure to seawater suggesting the intact cell walls are quite resistant to
429 diagenesis. Probably the epithelial cell walls and perithelial cell walls have differences in
430 the organic material that constrains the Mg uptake. The interfilament and intrafilament
431 (spaces between adjacent cell walls) calcification does not appear to be physically
432 constrained by an organic template [in the *P. onkodes* and *Clathromorphum Fosliefi*](#)
433 [\(Nash et al., 2013a; Adey et al., 2013\)](#). Mg-calcite crystals are randomly orientated or
434 roughly parallel to the cell walls, which suggests that the controls on calcification and
435 consequently Mg incorporation may be different again for the interfilament calcification.
436 It seems most likely that the difference in the mol% MgCO₃ for the white crust compared
437 to the pigmented new growth is due to organism-constrained Mg uptake during the crust
438 development. It cannot be determined from this study whether the Mg is incorporated in
439 its final concentrations as the new cell wall and inter/intra filament calcification is first
440 formed or if there is subsequent Mg enrichment over days/weeks/ months. However,
441 previous work subsampling portions of the CCA crust from the top to the base has not
442 demonstrated any systematic increase in mol% MgCO₃ (Nash et al., 2013b) suggesting if
443 there is post-deposition Mg enrichment, it occurs relatively contemporaneously with
444 growth.

445
446

447 The consistency of [Mg composition](#) across *P. onkodes* and new settlement CCA from
448 pre-industrial to high CO₂ treatments does not provide support for the theory that Mg-C
449 organisms will take up less [Mg](#) under higher CO₂ conditions (Andersson et al., 2008).
450 Instead our results agree with the response of *P. onkodes* in an 8 week laboratory
451 aquarium experiment which also showed no change in mol% MgCO₃ in pigmented
452 growth with CO₂ levels up to 1225 μ atm (Diaz-Pulido et al., 2014). Those CCA were not
453 embedded in resin and were grown in higher temperatures (28 and 30 degrees). Both
454 these aquarium experimental results are in agreement with new settlement CCA in CO₂
455 enriched flow through systems (Kuffner et al., 2008). This consistency of mol% MgCO₃
456 suggests there is a strong biological control on [Mg uptake](#) under variable CO₂

Rob Nash 6/20/15 4:30 PM

Moved up [1]: (Nash et al., 2013a; Adey et al., 2013)

Rob Nash 6/20/15 4:30 PM

Moved (insertion) [1]

Rob Nash 6/20/15 4:40 PM

Deleted: magnesium

Rob Nash 6/20/15 4:41 PM

Deleted: magnesium

Rob Nash 6/20/15 4:41 PM

Deleted: magnesium

462 concentrations and no detectable plastic response to CO₂ within the experimental ranges.
463 The absence of change across treatments for mol% MgCO₃ in the new settlement CCA,
464 none of which have dolomite, suggests that the similar apparent lack of response of the
465 mol% MgCO₃ in the white crusts to CO₂ treatments is unrelated to the presence of
466 dolomite. The lack of difference between pre-industrial, medium and high treatments in
467 the 6 month crust sample set suggests that no trends have been missed with the absence
468 of the control group.

469

470 4.2 Comparison to other studies

471 | The results from the *P. onkodes* are in contrast to the decreased Mg composition for
472 tropical branching *Neogoniolithon* sp. (Ries 2011). This form of *Neogoniolithon* is not
473 abundant in the high-energy environments that *P. onkodes* dominates. However, the
474 mol% MgCO₃ measured in the *Neogoniolithon* control (~18.7 - 21.3 mol% MgCO₃) was
475 much higher and with greater range than that measured for *P. onkodes* in this experiment
476 (pre-experimental crust 17.2-17.9, 3 month crust 16-16.8, new settlement 14.4-15.3
477 mol% MgCO₃ Supplement tables 1, 3 and 4). The mol% MgCO₃ in the *Neogoniolithon*
478 decreased to 18.7-16.7 mol% at 903 μatm CO₂ (equivalent CO₂ levels as our highest
479 treatment) but only decreased by another 1.3 mol% MgCO₃ on average (range 17.3-16.0
480 mol% MgCO₃) with an extra 1962 μatm (2865 μatm CO₂). Thus the lowest Mg levels
481 for the *Neogoniolithon* in the highest CO₂ treatments were comparable to our results for
482 control (and treatments) and to other *P. onkodes* collected from the Great Barrier Reef
483 (Nash et al., 2011; Diaz-Pulido et al., 2014). This raises the possibility that CCA Mg-C
484 levels are susceptible to change as CO₂ rises but only for levels higher than a stable
485 baseline, which for the tropical corallines may be in the range of ~16-17.5 mol%
486 MgCO₃. Egilisdottir et al., (2012) working on the temperate articulated coralline
487 *Corallina elongata* reported a significant decrease in Mg content for new structures
488 formed under CO₂ 550-1000 μatm. For tips, branches and basal parts formed under the
489 enriched CO₂, Mg content ranged from 14.7 – 15.9 mol% MgCO₃ and was not
490 significantly different from controls (15.7, 15.2, 15.4 mol% MgCO₃ respectively). On
491 the other hand, structures growing off the base exhibited 16 % MgCO₃ under control
492 conditions but reduced in the tips, branches and basal plates of these new structures (15.1,

Rob Nash 6/20/15 4:41 PM

Deleted: magnesium

494 14.9, 15.3 mol% MgCO₃) at 550 μatm CO₂. These results suggest there is a different
495 calcification process for the new structures compared to the tips, branches and basal parts
496 and that this calcification process is sensitive to CO₂ but only up to 550 μatm. Research
497 on temperate coralline *Lithothamnion glaciale* showed no change in [Mg] for new growth
498 over 80 days in reduced pH 7.7 treatments (Kamenos et al., 2013).

Neal Cantin 6/15/15 10:04 AM

Deleted: d

499
500 Work on CO₂ influences on coralline algae structure has to date been on temperate
501 corallines (e.g. Burdett et al., 2012; Egilisdottir et al., 2012; Ragazzola et al., 2012, 2013;
502 Hofmann et al., 2012; Kamenos et al., 2013). Experiments on living tropical CCA
503 calcification have focused on weight changes (e.g. Anthony et al., 2008; Comeau et al.,
504 2013; Johnson et al., 2014) and impacts on existing crust mineralogy (Diaz-Pulido et al.,
505 2014). There is little specific information known about calcification processes in tropical
506 crustose corallines. However, as this study and previous studies on mineralogy (Nash et
507 al., 2011, 2013b; Diaz-Pulido et al., 2014) show, carbonates in CCA are not only Mg-
508 calcite but can also include dolomite, magnesite and aragonite. It is clear that the net
509 mass of CCA is a result of multiple mineral-forming processes. While all form within the
510 biological structure it seems unlikely that infill dolomite, magnesite and aragonite are all
511 the result of organism controlled calcification processes and instead are biologically
512 induced. Thus experimental net weight changes for *P. onkodes* may not always be a
513 reflection of changes for only Mg-calcite calcification and/or dissolution.

514
515 Aragonite can form as a result of parasitic endolithic bacterial activity within the CCA
516 (Diaz-Pulido et al., 2014) and contribute to measured weight gain. In the Diaz-Pulido et
517 al., study (2014) weight change was due in part to a mix of bacterial-driven carbonate
518 destruction processes and abiotic aragonite precipitation as a result of calcium
519 mobilisation by the endolithic bacteria. In the Johnson et al., (2014) study weight gain by
520 CCA from locations downstream of the reef front was interpreted as indicating
521 acclimatisation. However, if there were more endolithic bacteria present in their
522 downstream CCA than the reef front CCA, it is possible that the experimental fluctuating
523 conditions with elevated CO₂ activated bacterial processes and the lower CO₂ resulted in
524 increased re-precipitation of mobilised calcium as aragonite (aragonite re-precipitation

526 transforms the porous crust to dense cement) which could account for a proportion of the
527 weight gain. Therefore, it is problematic to presume acclimatisation based on weight gain
528 without knowing how the weight was gained. The published experiments referred to in
529 this discussion were all conducted prior to the discovery of dolomite, magnesite and
530 aragonite in *P. onkodes*, but future studies should consider the more complex nature of
531 mineral composition of *P. onkodes* when attempting to explain weight changes and
532 calcification (e.g. Nash et al., 2013).

Rob Nash 6/9/15 5:44 PM

Deleted: CCA

533
534 The varied responses of the tropical and temperate corallines to altered CO₂ indicate that
535 the uptake of Mg by CCA is not consistent across all species or even within the same
536 organism (Egilsdottir et al., 2012). Furthermore, the use of different methods of
537 measuring Mg concentration potentially complicates comparisons across data sets. Ries
538 (2011) and our study used XRD to determine mol% MgCO₃. This measurement only
539 returns mol% for the Mg-Calcite component and is not influenced by the presence of Mg
540 in other forms, e.g. dolomite or within organics, or diluted by the presence of aragonite.
541 Kamenos et al., (2013) used Raman spectroscopy for identifying mol% MgCO₃ changes,
542 this method is not widely used for coralline algae mineralogy studies. Egilsdottir et al.,
543 (2012) used inductively coupled plasma- atomic emission spectroscopy (ICP-AES) to
544 quantify bulk Mg and Ragazzola et al., (2013) used electron microprobe to obtain an
545 average elemental composition for Mg/Ca ratios. These methods return bulk Mg for the
546 total sample or portion under the electron beam and may be skewed by undetected
547 aragonite, common in corallines (Smith et al., 2012; Nash et al., 2013b) or presence of
548 Mg not within the Mg-calcite, (e.g. Caragnano et al., 2014).

Rob Nash 6/20/15 4:42 PM

Deleted: magnesium

Rob Nash 6/20/15 4:43 PM

Deleted: magnesium

Rob Nash 6/20/15 4:43 PM

Deleted: magnesium

Rob Nash 6/20/15 4:43 PM

Deleted: magnesium

550 4.3 Dolomite formation within 12 weeks

551 Prior to the discovery of bio-mediated dolomite in association with bacteria (Vasconcelos
552 and Mackenzie 1997) and CCA (Nash et al., 2011,) dolomite was thought to form by
553 chemical alteration of limestone over geological time frames, e.g. thousands to millions
554 of years (e.g. Saller 1984). Although it has also been controversially argued that
555 dolomite was the primary precipitation in some ancient dolomite formations (Tucker
556 1982). Our experimental results demonstrate that bio-mineralised dolomite formation is

562 rapid and occurring contemporaneously with the surrounding limestone formation. The
563 apparent reduction in dolomite formation in the experimental conditions compared to the
564 pre-experimental growth indicates that there is also a rapid response to changing
565 environmental conditions. Accordingly, any interpretation of past environments made
566 using dolomite that may have had a biological origin, i.e. dolomite in formerly shallow
567 tropical environments, would need to take into account this potentially rapid formation
568 and response to environmental change.

569

570 **4.4 Implications for interpreting the geological past**

571 The absence of a significant effect of CO₂ on dolomite formation in this experiment
572 suggests that the observed correlation in the geologic rock record of dolomite and
573 greenhouse conditions may not be a direct result of high CO₂ driving increased primary
574 bio-mineralised dolomite formation. However, as noted in previous work (Nash et al.,
575 2013a; Diaz-Pulido et al., 2014) dolomite is more resistant to chemical dissolution and
576 biological erosion than Mg-calcite (and presumably also calcite). Therefore, the positive
577 correlation of dolomite and greenhouse epochs in the rock record (e.g. MacKenzie et al.,
578 2008; Wilkinson and Given 1986) may be due in part to preferential preservation of bio-
579 mineralised dolomite compared to surrounding skeletal material, rather than CO₂ or
580 temperature driven biological processes leading to increased dolomite formation.

581 Furthermore, during greenhouse times, sea level was higher thereby providing greater
582 area of warm shallow (epeiric) seas and thus more accommodation space for calcifying
583 algae that may have formed dolomite. While past primary bio-mineralised dolomite
584 levels may not have been directly linked to CO₂ levels, there is certainly support from
585 other work (Nash et al., 2013a; Diaz-Pulido et al., 2014) for indirect biologically-
586 associated processes leading to increased abundance of bio-mineralised dolomite under
587 higher CO₂ conditions.

588

589 **4.5 Changes in calcification in experimental tanks**

590 Considering the aragonite observed in the crust where the CCA was transferred to the
591 experimental tanks, it may be that interruptions to normal growth after transfer to
592 experimental tanks, allowed seawater to penetrate into the shallow surface layer resulting

593 in alteration of Mg-C to aragonite. Previous experiments on calcification rates of CCA
594 found that rates of photosynthesis, and production of inorganic and organic carbon, were
595 significantly lower in experimental tanks than *in situ* (Chisholm, 2003). A decrease in
596 photosynthesis and calcification rates may be the explanation for the observed differences
597 in calcified crust in this study, although the exact mechanism leading to the change is not
598 known. The absence of the organic film in the experimental growth (Fig. 5c) raises the
599 possibility that it is the absence of these organics that has led to the observed differences
600 in calcification. This organic film is consistently present on the pre-experimental growth
601 and consistently absent from the experimental growth. Thus it is unlikely to be a sample
602 preparation artifact, although the preparation method may make this film more readily
603 visible than if the samples had been fractured leaving an uneven surface. Reduced
604 organic production may also lead to less dolomite as experiments have shown that
605 dolomite nucleates on polysaccharides produced by red algae (Zhang et al., 2012). It is
606 probable that our experimental results understate how much dolomite could be formed in
607 the open marine environment over a 3 and 6 month period.

608

609 The observation that the change to experimental tanks coincided with changes in CCA
610 calcification has implications for extrapolating experimental results back to the natural
611 environment. There is a substantial change in the ultrastructure and secondary
612 mineralisation (i.e. formation of dolomite) processes. While comparisons between
613 treatments are reliable, exact rates of calcification for *P. onkodes* are likely to be
614 understated in experimental conditions compared to the open reef. This is an area that
615 requires further work to determine what is causing this difference in calcification and if it
616 is common to all similar experiments. Flow and wave energy will be important factors
617 that influence the calcification processes and should also be considered in future
618 aquarium designs that seek to test the effects of future acidification scenarios on CCA's.

619

620 | **4.6 What does Mol% Mg-calcite mean for the CCA physiology and reef** 621 **processes in a changing climate?**

622 | There have been no studies to date that explore the drivers of organism-controlled
623 calcification in the key reef-builder *P. onkodes* and what role the Mg content plays in

Rob Nash 6/20/15 4:45 PM

Deleted:

Rob Nash 6/9/15 5:44 PM

Deleted: C

Rob Nash 6/9/15 5:45 PM

Deleted: which

Rob Nash 6/9/15 5:45 PM

Deleted:

628 this. Thus it is unclear at this time what influence the mol% MgCO₃ has on CCA
629 physiology and reef processes and even more difficult to anticipate what may happen in
630 the future in a changing climate. Early studies on Mg-C CCA dissolution rates (Plummer
631 and Mackenzie 1974; Bischoff et al., 1987) used CCA that had dolomite and possibly
632 magnesite (see Nash et al., 2013 for discussion). Those results were a mix of dissolution
633 rates for the 2-3 different Mg minerals, not just for Mg-calcite with different phases of
634 mol% MgCO₃ as was interpreted. Much of our present understanding of biogenic Mg-C
635 dissolution is based on those interpretations (e.g. Andersson et al., 2008). Considering
636 how recent work on CCA dissolution has revealed that a complex suite of interacting
637 mineral, biological, bacterial and chemical factors contribute to net dissolution responses
638 (Nash et al., 2013; Reyes-Nivia et al., 2014; Diaz-Pulido et al., 2014) it has become
639 apparent that the prevailing theory that higher Mg content leads to lower stability is
640 probably not applicable to tropical *P. onkodes*. Indeed there have been no dissolution
641 experiments comparing the dissolution rates of CCA with different mol% MgCO₃ to test
642 the correlation of dissolution rates to Mg content of Mg-C.

Rob Nash 6/20/15 4:46 PM

Deleted: therefore

Rob Nash 6/20/15 4:46 PM

Deleted: t

Rob Nash 6/20/15 4:46 PM

Deleted: magnesium

Rob Nash 6/9/15 5:45 PM

Deleted: CCA

Rob Nash 6/20/15 4:47 PM

Deleted: magnesium

Neal Cantin 6/15/15 10:24 AM

Deleted: . .

644 4.7 Implications for reef management

645 Finding that dolomite is not affected by ocean acidification in these 3 and 6 month
646 experiments is good news for the survival of CCA species *P. onkodes* under predicted
647 ocean acidification conditions. Dolomite confers stability on the CCA and facilitates its
648 reef-building role (Nash et al., 2013a) as well as being resistant to bacterial bio-erosion
649 (Diaz-Pulido et al., 2014). At this time exact drivers of CCA dolomite formation have not
650 been identified. It seems most likely that dolomite formation is related to provision of a
651 suitable organic substrate, probably being the polysaccharides derived from red algae for
652 agar (Nash et al., 2013a; Zhang et al., 2012). For coral reef management, it is necessary
653 to understand what environmental conditions negatively impact dolomite formation.
654 CCA crust formation is likely to suffer negative affects from reduced recruitment,
655 increased bleaching, bio-erosion and dissolution under higher CO₂ and temperatures
656 (Kuffner et al., 2011; Diaz-Pulido et al., 2012). However, understanding the conditions
657 that negatively impact dolomite formation may enable more effective assessments of the
658 risk that CO₂-driven ocean acidification may pose to important reef-builders such as *P.*

665 *onkodes*. Identifying the drivers and constraints of CCA dolomite formation is an area of
666 research that has not yet been initiated and as such, there is a long way to go to
667 understand what conditions may negatively impact on CCA dolomite formation.

668

669 **Acknowledgements**

670 Thanks to Frank Brink and the Centre for Advanced Microscopy at the Australian
671 National University for assistance with SEM. Thanks to Florita Flores, Michelle Liddy,
672 Julia Strahl, Paulina Kaniewska and Jordan Hollarsmith for aquarium maintenance and
673 experimental assistance. Funding for the experimental work was provided by the
674 Australian Institute of Marine Science and a Super Science Fellowship from the
675 Australian Research Council. Support for mineral analysis was provided by the
676 Electronic Materials Engineering department at the Research School of Physics,
677 Australian National University.

678

679

680

681 **References**

682

683

684 Adey, W. H., Halfar, J., and Williams, B.: The coralline genus *Clathromorphum* Foslie
685 emend. Adey: Biological, physiological, and ecological factors controlling
686 carbonate production in an Arctic-Subarctic climate archive. *Smithsonian*
687 *contributions to the marine sciences*; number 40, 2013.

688

689 Andersson, A. J., Mackenzie, F. T., Bates, N. R.: Life on the margin: implications of
690 ocean acidification on Mg-calcite, high latitude and cold-water marine calcifiers,
691 *Mar. Ecol. Prog. Ser.* 373, 265-273, 2008.

692

693 Anthony, K. R. N., Kline, D. I., Diaz-Pulido, G., Dove, S., Hoegh-Guldberg, O.: Ocean
694 acidification causes bleaching and productivity loss in coral reef builders, *PNAS*
695 105, 17442-17446, 2008.

Rob Nash 6/20/15 4:37 PM

Deleted:

697
698 Bischoff, W. D., Mackenzie, F. T., Bishop, F. C.: Stabilities of synthetic magnesian
699 calcites in aqueous solution: Comparison with biogenic materials, *Geochim.*
700 *Cosmochim. Acta.* 51, 1413–1423, 1987.
701
702 Burdett, H. L., Hennige, S. J., Francis, F. T. Y., and Kamenos, N. A.: The photosynthetic
703 characteristics of red coralline algae, determined using pulse amplitude
704 modulation (PAM) fluorometry, *Mar. Biol. Res.*, 8, 756-763, 2012.
705
706 Caragnano, A. D., Basso, D. E., Jacob, D., Storz, G., Rodondi, F., Benzoni, Dutrieux, E.:
707 The coralline red alga *Lithophyllum kotschyianum* f. *affine* as proxy of climate
708 variability in the Yemen coast, Gulf of Aden (NW Indian Ocean), *Geochim*
709 *Cosmochim Ac*
710 124,1-17, 2014.
711
712 Chisholm, J. R. M., Primary productivity of reef-building crustose coralline algae,
713 *Limnol. Oceanogr.* 48,1376-1387, 2003.
714
715 Comeau, S., Edmunds, P. J., Spindel, N. B., Carpenter, R. C.: The responses of eight
716 coral reef calcifiers to increasing partial pressure of CO₂ do not exhibit a tipping
717 point, *Limnol. Oceanogr.* 58, 388-398, 2013.
718
719 Darrenougue, N., De Deckker, P., Eggins, S., & Payri, C: Sea-surface temperature
720 reconstruction from trace elements variations of tropical coralline red algae.
721 *Quaternary Science Reviews*, 93, 34-46, 2014.
722
723 Diaz-Pulido, G., Anthony, K., Kline, D. I., Dove, S., Hoegh-Guldberg, O.: Interactions
724 between ocean acidification and warming on the mortality and dissolution of
725 coralline algae, *J. Phyc.* 48, 32-39, 2012.
726

Rob Nash 6/20/15 4:37 PM

Deleted:

728 Diaz-Pulido, G., Nash, M. C., Anthony, K. R. N., Bender, D., Opdyke, B. N., Reyes-
729 Nivia, C., Troitzsch, U.: Greenhouse conditions induce mineralogical changes and
730 dolomite accumulation in coralline algae on tropical reefs, *Nat Comms*, 5,2014.
731
732 Egilsdottir, H., Noisette, F., Noel, L. M., Olafsson, J., Martin, S.: Effects of pCO₂ on
733 physiology and skeletal mineralogy in a tidal pool coralline alga *Corallina*
734 *elongate*, *Mar Biol*, 160, 2103-2112, 2012.
735
736 Fietzke, J., Ragazzola, F., Halfar, J., Dietze, H., Foster, L. C., Hansteen, T. H.,
737 Eisenhauer, A., and Steneck, R. S.: Century-scale trends and seasonality in pH
738 and temperature for shallow zones of the Bering Sea. *P. Natl. Acad. Sci.*, 112,
739 2960-2965, 2015
740
741 Gaines, A.: Protodolomite redefined, *J. Sed. Pet.*, 47, 543-546, 1977
742
743 Given, R. K., Wilkinson, B. H.: Dolomite abundance and stratigraphic age: constraints on
744 rates and mechanisms of Phanerozoic dolostone formation, *J Sediment Petrol* 57,
745 1068-1078, 1987.
746
747 Halfar, J., Adey, W. H., Kronz, A., Hetzinger, S., Edinger, E., and Fitzhugh, W. W.:
748 Arctic sea-ice decline archived by multicentury annual-resolution record from
749 crustose coralline algal proxy. *P. Natl. Acad. Sci.*, 110, 19737-19741, 2013.
750
751 Hofmann, L. C., Yildiz, G., Hanelt, D., Bischof, K.: Physiological responses of the
752 calcifying rhodophyte, *Corallina officinalis* (L.), to future CO₂ levels, *Mar Biol*,
753 159, 783-792, 2012.
754
755 Howard, W. R., Nash, M., Anthony, K., Schmutter, K., Bostock, H., Bromhead, D., ...
756 Williamson, J.: Ocean acidification. *In A Marine Climate Change Impacts and*
757 *Adaptation Report Card for Australia 2012*, Edited by Poloczanska E, Hobday A,

758 Richardson A. Centre for Australian Weather and Climate Research, Hobart,
759 TAS,2012.
760
761 Jones, B., Luth, R. W., McNeil, A. J.: Powder X-ray diffraction analysis of homogeneous
762 and heterogeneous sedimentary dolostones, *J. Sed. Res.* 71, 790-799, 2001.
763
764 Johnson, M. D., Moriarty, V. W., Carpenter, R. C.: Acclimatization of the Crustose
765 Coralline Alga *Porolithon onkodes* to variable pCO₂, *PLoS ONE* 9, e87678,
766 2014.
767
768 Kaczmarek, S. E., and Sibley, D. F.: On the evolution of dolomite stoichiometry and
769 cation order during high-temperature synthesis experiments: An alternative model
770 for the geochemical evolution of natural dolomites, *Sed. Geol.* 240, 30-40, 2011.
771
772 Kamenos, N. A., Cusack, M., and Moore, P. G.: Coralline algae are global
773 palaeothermometers with bi-weekly resolution. *Geochim. Cosmochim.*
774 *Acta*, 72(3), 771-779, 2008.
775
776 Kamenos, N. A., Burdett, H. L., Aloisio, E., Findlay, H. S., Martin, S., Longbone, C.,
777 Dunn, J., Widdicombe, S., and Calosi, P.: Coralline algal structure is more
778 sensitive to rate, rather than the magnitude, of ocean acidification, *Global Change*
779 *Biology*, 19, 3621-3628, 2013.
780
781 Kuffner, I. B., Andersson, A. J., Jokiel, P. L., Rodgers, K. S., Mackenzie, F. T.:
782 Decreased abundance of crustose coralline algae due to ocean acidification, *Nat*
783 *Geoscience*, 1, 114-117, 2007.
784
785 Morse, J. W., Arvidson, R. S., Lüttge, A.: Calcium carbonate formation and dissolution,
786 *Chem Rev*, 107, 342-381, 2007.
787

788 Nash, M. C., Troitzsch, U., Opdyke, B. N., Trafford, J. M., Russell, B. D., Kline, D.
789 I.: First discovery of dolomite and magnesite in living coralline algae and its
790 geobiological implications, *Biogeosciences*, 8, 3331-3340, 2011.
791

792 Nash, M. C., Opdyke, B. N., Troitzsch, U., Russell, B. D., Adey, W. H., Kato, A., ...
793 Kline, D. I., Dolomite-rich coralline algae in reefs resist dissolution in acidified
794 conditions, *Nat Climate Change*, 3, 268-272, 2013a.
795

796 Nash, M. C., Opdyke, B. N., Wu, Z., Xu, H., Trafford, J. M.: Simple x-ray diffraction
797 techniques to identify mg-calcite, dolomite, and magnesite in tropical coralline
798 algae and assess peak asymmetry, *J Sediment Res* 83, 1085-1099, 2013b.
799

800 Pueschel, C. M., Judson, B. L., and Wegeberg, S. : Decalcification during epithelial cell
801 turnover in *Jania adhaerens* (Corallinales, Rhodophyta). *Phycologia*, 44, 156-162,
802 2005.
803

804 Ramirez-Reinat, E. L., and Garcia-Pichel, F.: Characterization of a marine
805 cyanobacterium that bores into carbonates and the redescription of the genus
806 *Mastigocoleus*, *J. Phycol.* 48, 740-749, 2012.
807

808 Ries, J. B.: Skeletal mineralogy in a high CO₂ world, *J. Exp. Mar. Biol. Ecol.* 403, 54-64,
809 2011.
810

811 Mackenzie, F. T., Arvidson, R. S., Guidry, M. W.: Chemostatic models of the ocean
812 atmosphere-sediment system through Phanerozoic time, *Mineral Mag.* 72, 329-
813 332, 2008.
814

815 Orr, J.: Recent and future changes in ocean carbonate chemistry, in *Ocean Acidification*
816 (eds Gattuso JP, Hansson L) Chpt 3, 41-66, 2011.
817

818 Plummer, L. N., Mackenzie, F. T.: Predicting mineral solubility from rate data:
819 Application to the dissolution of magnesian calcites, *Am. J. Sci.* 274, 61–83,
820 1974.
821

822 Ragazzola, F., Foster, L. C., Form, A., Anderson, P. S., Hansteen, T. H., Fietzke, J.:
823 Ocean acidification weakens the structural integrity of coralline algae, *Glob*
824 *Change Biol*, 18, 2804-2812, 2012.
825

826 Ragazzola, F., Foster, L. C., Form, A. U., Buscher, J., Hansteen, T. H., Fietzke, J.:
827 Phenotypic plasticity of coralline algae in a high CO₂ world, *Ecol Evol* 3, 3436-
828 3446, 2013.
829

830 Reyes-Nivia, C., Diaz-Pulido, G., Dove, S.: Relative roles of endolithic algae and
831 carbonate chemistry variability in the skeletal dissolution of crustose coralline
832 algae, *Biogeosciences Discussions* 11, 2993-3021, 2014.
833

834 Saller, A. H.: Petrologic and geochemical constraints on the origin of subsurface
835 dolomite, Enewetak Atoll: An example of dolomitization by normal seawater,
836 *Geology*, 12, 217-220. 1984.
837

838 Smith, A. M., Sutherland, J. E., Kregting, L., Farr, T. J., Winter, D. J.: Phylomineralogy
839 of the Coralline red algae: Correlation of skeletal mineralogy with molecular
840 phylogeny, *Phytochemistry*, 81, 97-108, 2012.
841

842 Steneck, R. S.: The ecology of coralline algal crusts: convergent patterns and adaptative
843 strategies. *Annual Review of Ecology and Systematics*, 273-303, 1986.
844

845 Tucker, M. E.: Precambrian dolomites: petrographic and isotopic evidence that they
846 differ from Phanerozoic dolomites, *Geology*, 10, 7-12, 1982.
847

- 848 Uthicke, S., Pecorino, D., Albright, R., Negri, A. P., Cantin, N., Liddy, M., Dworjanyn,
849 S., Kamyra, P., Byrne, M., Lamare, M.: Impacts of Ocean Acidification on Early
850 Life-History Stages and Settlement of the Coral-Eating Sea Star *Acanthaster*
851 *planci*, PLoS ONE 8, e82938, 2013.
- 852
- 853 Vasconcelos, C., McKenzie, J. A.: Microbial mediation of modern dolomite precipitation
854 and diagenesis under anoxic conditions (Lagoa Vermelha, Rio de Janeiro, Brazil),
855 J Sediment Res, 67, 378-390, 1997.
- 856
- 857 Wilkinson, B. H., Given, R. K.: Secular variation in abiotic marine carbonates:
858 Constraints on Phanerozoic atmospheric carbon dioxide contents and oceanic
859 Mg/Ca ratios, J. Geol, 94, 321-333, 1986.
- 860
- 861 Zhang, F., Xu, H., Konishi, H., Shelobolina, E. S., Roden, E. E.: Polysaccharide-
862 catalyzed nucleation and growth of disordered dolomite: A potential precursor of
863 sedimentary dolomite, Am Mineral, 97, 556-567, 2012.
- 864
- 865 Zhang, F., Xu, H., Shelobolina, E. S., Konishi, H., Converse, B., Shen, Z., and Roden, E.
866 E.: The catalytic effect of bound extracellular polymeric substances excreted by
867 anaerobic microorganisms on Ca-Mg carbonate precipitation: Implications for the
868 “dolomite problem”. Am. Mineral.,100, 483-494, 2015.
- 869
- 870 Zhao, H., and Jones, B.: Origin of “Island dolostones”: a case study from the Cayman
871 Formation (Miocene), Cayman Brac, British West Indies, Sed. Geol. 243-244,
872 191-206, 2012.
- 873
- 874

875 **Figure Legends**

876 **Table 1:** Two factor analysis of variance (ANOVA) testing for difference in mol%
877 MgCO₃ and Asymmetry indicating dolomite, between different CO₂ treatments (Factor
878 Treatment) and experimental growth versus pre-experimental growth (Factor Type). No

879 significant difference related to CO₂ treatments, but significant difference between
880 experimental and pre-experimental growth for both mol% MgCO₃ and dolomite
881 asymmetry.

882 | **Figure 1:** Example of *P. onkodes* after 3 months. New pigmented crust overgrowing
883 resin used for XRD.

884 **Figure 2:** Magnesium composition for experimental growth of *P. onkodes*. Mol% is for
885 Mg-calcite mol% MgCO₃. Asymm mol% includes influence of dolomite asymmetry on
886 calculated Mg-calcite mol% MgCO₃, the more dolomite present the higher the Asymm
887 mol%. **(a)** New crust after 3 months. **(b)** New crust after 6 months. There was no
888 significant difference between treatments for either the mol% MgCO₃ or the Asymm
889 mol% in new crust after 3 or 6 months. 889 ~~Δ~~ control samples were unavailable for
890 mineral analyses. **(c)** New settlement after 6 months. As for the new crust, there was no
891 significant difference across the treatments in mol % MgCO₃. There is no dolomite in the
892 new settlement consistent with the absence of white crust. Error bars are ± 1 s.d.

893 **Figure 3:** Magnesium composition for CCA new settlement, 3 month crust, 6 month
894 crust, and pre-experimental crust. The mol% MgCO₃ in the Mg-calcite increases from
895 new settlement to 3 and 6 months, and again for the pre-experimental crust. Dolomite is
896 not present in the new settlement, appears within 3 months, increases in amount in the 6
897 month new crust, but is highest in the pre-experimental crust. Error bars are 1 s.d.

898 **Figure 4:** SEM (Backscatter -BSE) of control *P. onkodes* showing dolomite in
899 experimental and pre-experimental growth. BSE SEM shows the lighter elements i.e.
900 | magnesium, as darker gray and heavier elements, i.e. calcium ~~js~~ pale gray to white.
901 Secondary electron images show the topography of the sample but do not provide
902 information on the elemental composition. EDS measurements are made in the different
903 gray shade areas to measure Mg composition (range listed in supplement) and this is used
904 to identify the mineral composition. Once the measurements have been made it is
905 possible then to identify dolomite and calcite from the gray shade. **(a)** Experimental
906 growth- dolomite (D) Dolomite-composition material in cell. This is not the typical cell
907 lining but has been observed in other CCA. Mg-calcite (Mg-C). Scale = 2 microns. **(b)**

Rob Nash 6/9/15 6:05 PM

Deleted: Porolithon

Rob Nash 6/9/15 6:05 PM

Deleted: (CCA)

Rob Nash 6/9/15 6:05 PM

Deleted: are

911 Experimental growth: micro-scale lumpy dolomite lining cell. Scale = 1 micron. Cell
912 growth in experimental growth is less regular and organized than pre-experimental
913 growth. **(c)** Dolomite cell lining in pre-experimental growth. Notice the very narrow cell
914 walls. **(d)** Dolomite infill in a reproductive conceptacle in the old growth. Cells below
915 conceptacle are all in-filled with dolomite. Scale bars: a and c = 2 microns, b = 1 micron,
916 d = 10 microns.

917 **Figure 5:** Control *P. onkodes* with experimental growth on pre-experimental growth. **(a)**
918 (BSE) There is a visible difference in the appearance of experimental crust (black arrow)
919 to the pre-experimental growth (black dashed arrow). The lighter grey of the surface is
920 due to less magnesium (dolomite) infilling the cells that appear as darker grey infill in the
921 pre-experimental lower part of the crust. Black box enlarged in **b**. **D** is dolomitised
922 conceptacle. **(b)** Close up showing the consistent presence of infill in pre-experimental
923 growth whereas in the new growth regular dolomite cell lining is absent. Also, the Mg-C
924 crust itself appears to be less dense with many cracks from the cutting visible in the new
925 growth but not so in the pre-experimental growth. **(c)** Secondary electron image of
926 control CCA. The pre-experimental growth appears to have a fine opaque organic film
927 covering part of the cut crust (white dashed arrow), but this is not present in the
928 experimental growth (White arrow). **(d)** Control CCA (BSE) Dashed arrow to pre-
929 experimental growth. Grey cells are dolomite infill. Black arrow to experimental growth,
930 generally an absence of dolomite infill, note line of porosity in transition between pre-
931 experimental and experimental growth. Scale bars: a, c and d = 100 microns, b = 20
932 microns.

933 **Figure 6:** Transition from pre-experimental crust to experimental crust in *P. onkodes*,
934 pre-industrial CCA **(a, b)** (BSE), high CO₂ CCA **(c, d)**. Transition from pre-experimental
935 growth to experimental identified by following the growth lines from the crust on the
936 resin (not pictured) across the sample. **(a)** overview, brackets- new growth. **(b)** close up
937 of transition. Crust below dashed line is pre-experimental growth. Dolomite infills cells
938 (black arrows). Above dashed line new growth does not have cells infilled, crust has
939 been damaged by saw cut. **(c)** Overview of transition to new growth in high CO₂ CCA,
940 brackets – new growth. **(d)** close up of transition. Similarly to control and pre-industrial

941 CCA, cells in pre-experimental growth are infilled with dolomite (black arrows). Crust
 942 above dashed line grew during experiment. Cells are not infilled with dolomite and crust
 943 has crushed under the sawcut. Scale bars a, b, c and d = 20 microns. Close up of
 944 transition between from pre-experimental growth to experimental growth in supplement
 945 Fig. 3.

946 **Figure 7:** SEM (BSE) of Control *P. onkodes* (AC4). **(a)** Overview of experimental
 947 growth, pre-experimental growth and transition zone (bracket). Cells at the surface do
 948 not have dolomite. White box enlarged in B. **(b)** Cells in experimental growth have no
 949 dolomite infill. Cells below experimental growth have dolomite lining the cells but the
 950 centres are in-filled with aragonite. White box enlarged in C, black box enlarged in E. **(c)**
 951 close up of cell infill by aragonite within the dolomite lining. **(d)** Dolomite lined cell in
 952 transition zone with aragonite infill. **(e)** Patch of crust below experimental growth with
 953 aragonite infill. **(f)** Close up of dolomite-lined cell with aragonite infill. Scale bars: a and
 954 b = 20 microns, c and f = 1 micron, d = 2 microns, e = 10 microns.

955 **Figure 8:** SEM (BSE) of varied mineral fabrics in CCA. **(a)** Alteration of base of CCA
 956 crust by bacteria to aragonite (Diaz-Pulido et al., 2014), remnant CCA cells are visible in
 957 the aragonite (A) confirming it was CCA crust and not coral substrate. **(b)** Hypothallus
 958 cells grow parallel to substrate then grow vertically and are in-filled with dolomite (D).
 959 In-fill of micro-borer trace by aragonite and dolomite rim (arrow). **(c)** Band of dolomite
 960 between aragonite alteration and undamaged cells. **(d)** Damaged crust has been in-filled
 961 with new cell growth rich in dolomite. Scale bars: a = 100 microns, b, c and d = 20
 962 microns.

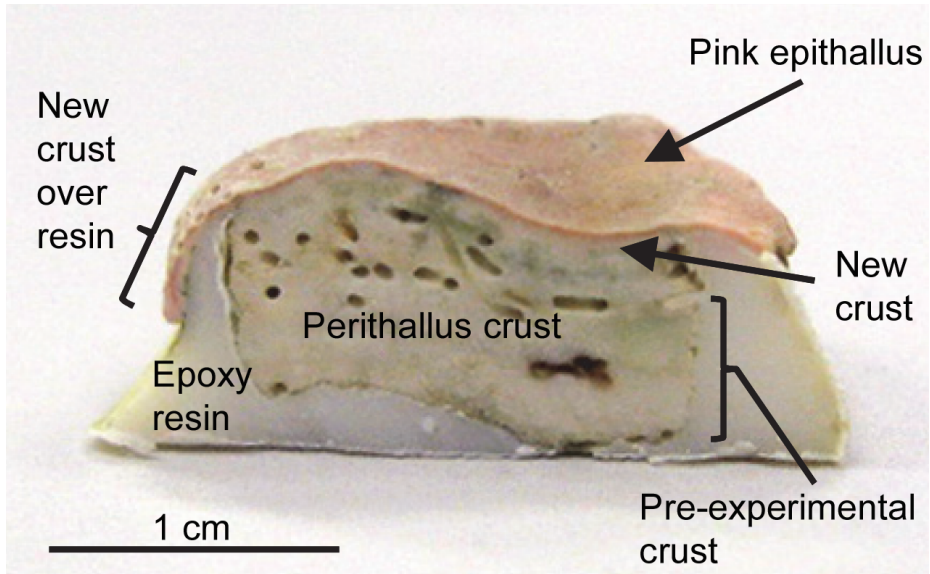
963
 964

	DF	Mol %			Asymmetry			
		MS	F	p	DF	MS	F	p
Treatment	2	1.76E-05	0.77	0.4754	2	1.98E-04	0.55	0.582
Type	1	6.52E-04	28.54	< 0.001	1	7.00E-03	19.57	<0.001
Tr X Type	2	0.49	0.61972	0.1195	2	0.35	0.7082	0.099

965

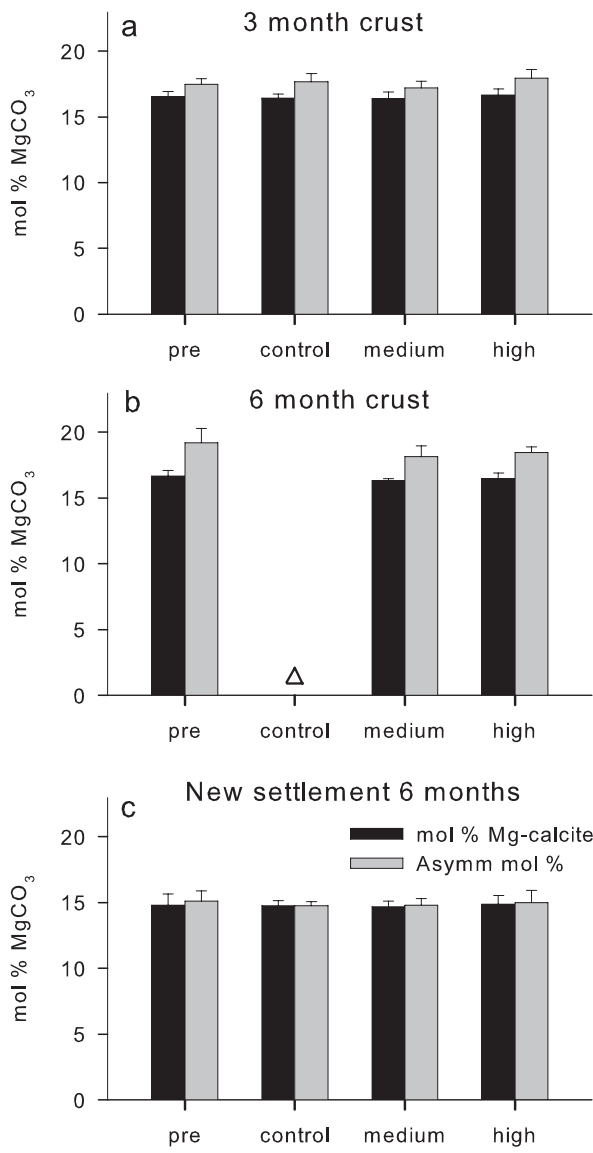
966 Table 1

967

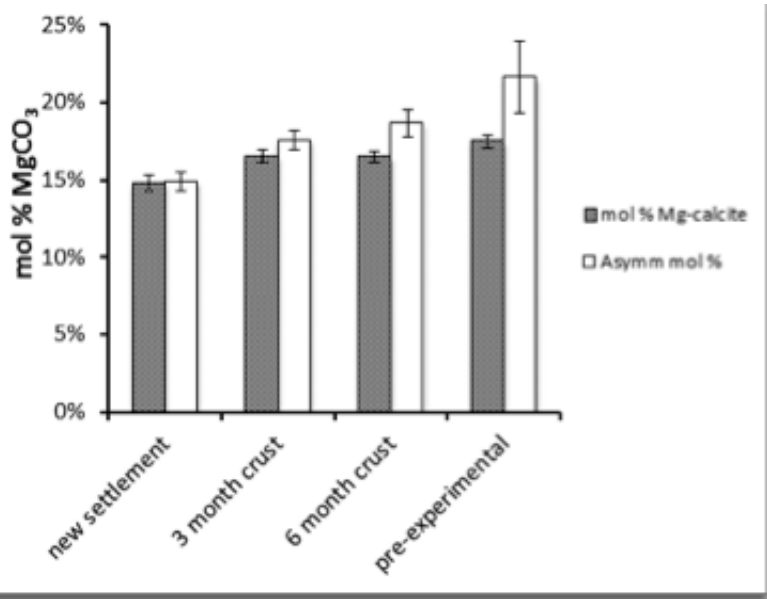


968

969 Figure 1



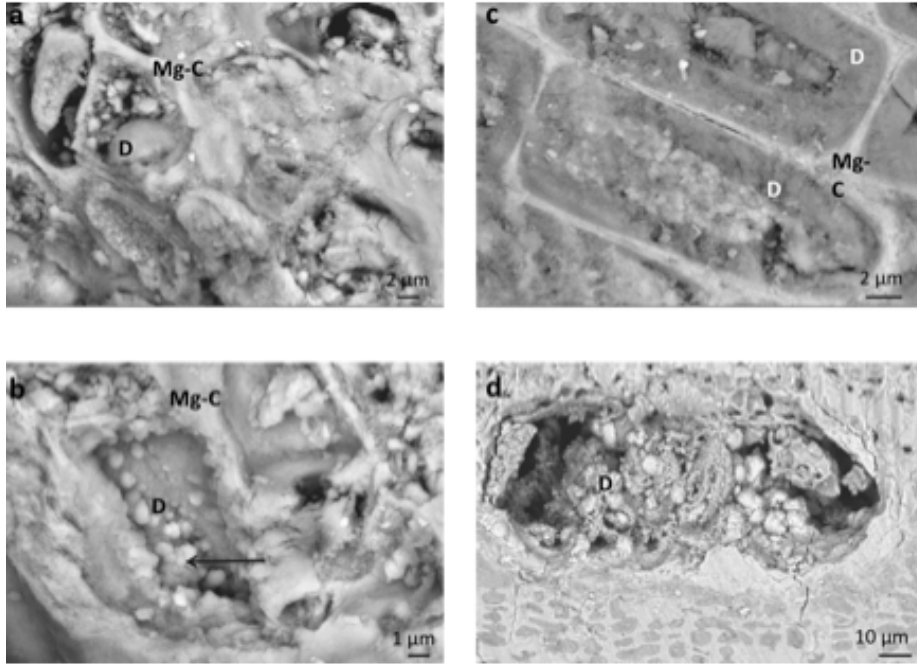
970
971 **Figure 2**



972

973

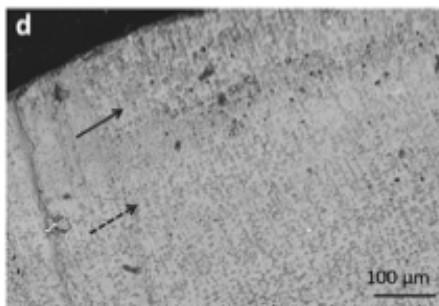
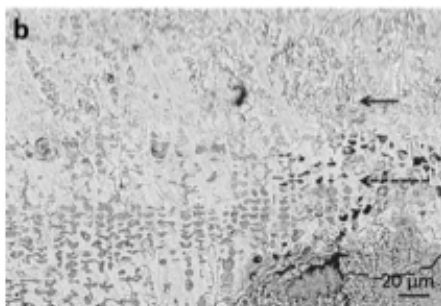
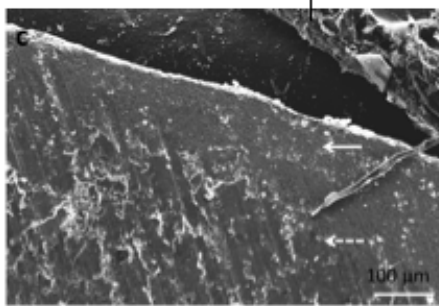
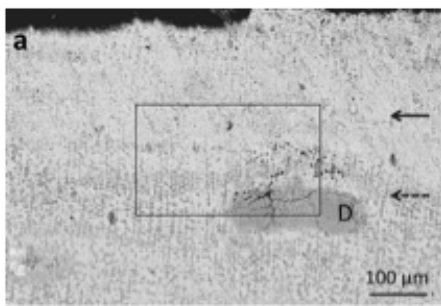
Figure 3



974

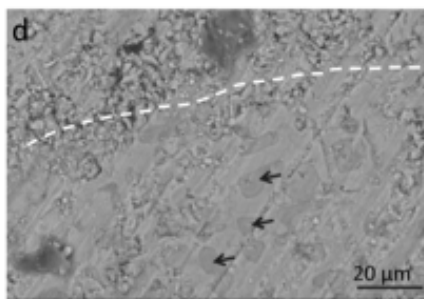
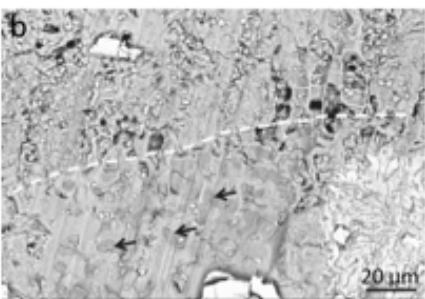
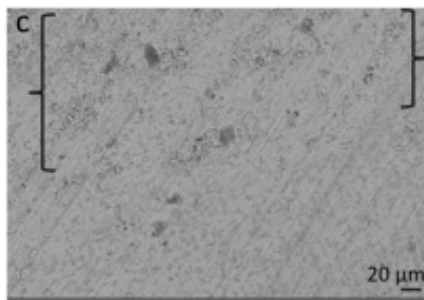
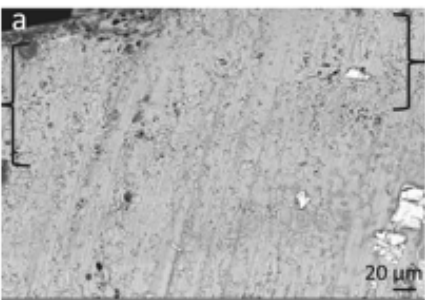
975

Figure 4



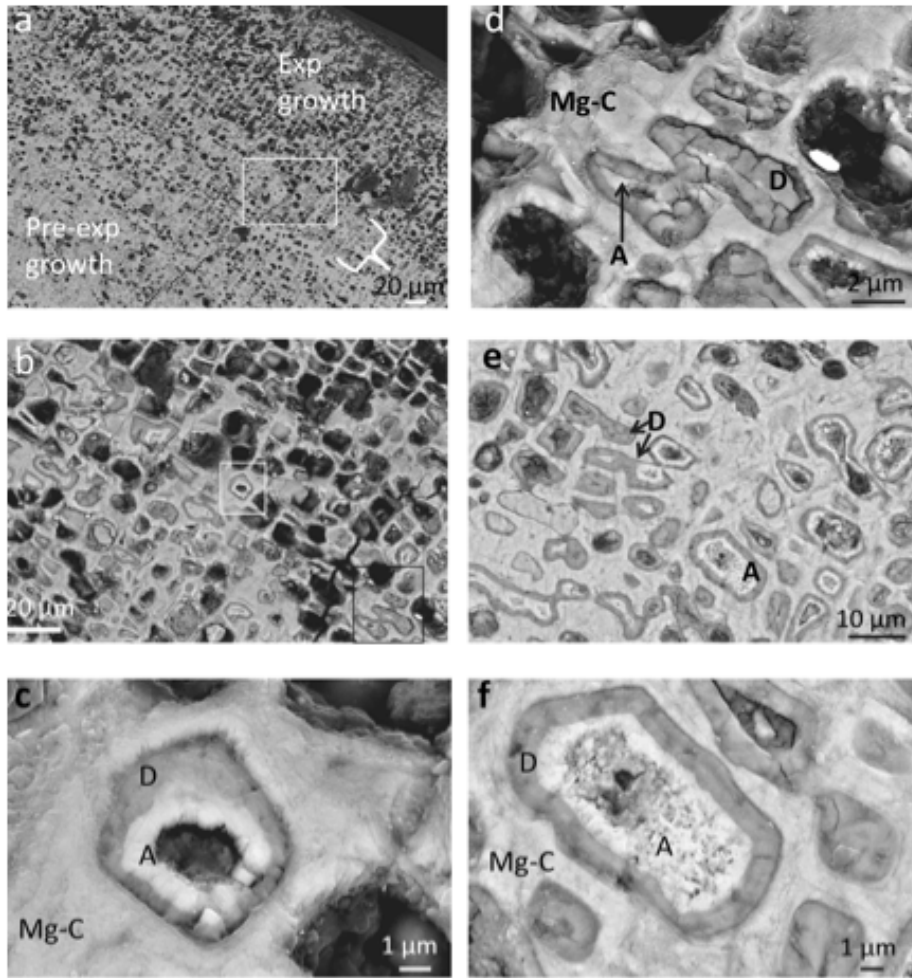
976
977

Figure 5

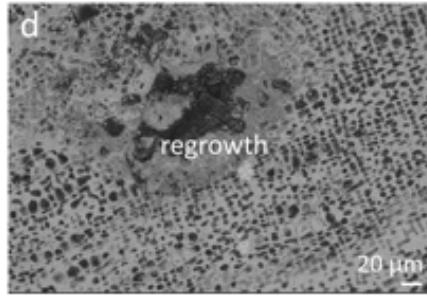
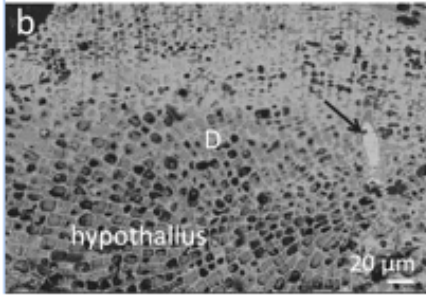
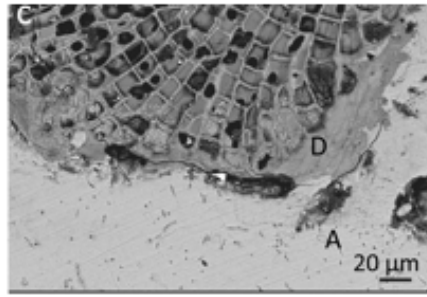
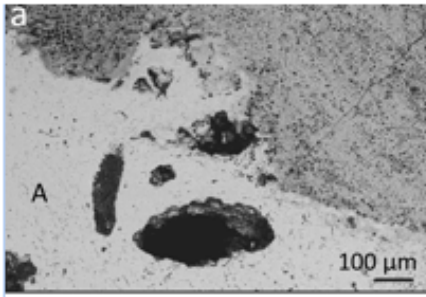


978

979 Figure 6



980
981 Figure 7



982
983

Figure 8